THE JOURNAL OF PHYSICAL CHEMISTRY C

ARTICLE

pubs.acs.org/JPCC

Thermoelectric Properties of Ultrasmall Single-Wall Carbon Nanotubes

X. J. Tan,[†] H. J. Liu,[*,†] Y. W. Wen,[†] H. Y. Lv,[†] L. Pan,[†] J. Shi,[*,†] and X. F. Tang[‡]

[†]Key Laboratory of Artificial Micro- and Nanostructures of Ministry of Education and School of Physics and Technology, Wuhan University, Wuhan 430072, China

[‡]State Key Laboratory of Advanced Technology for Materials Synthesis and Processing, Wuhan University of Technology, Wuhan 430072, China

ABSTRACT: The electronic transport of three kinds of ultrasmall single-wall carbon nanotubes are studied by using nonequilibrium Green's function method. It is found that the transmission function displays a clear stepwise structure that gives the number of electron channels. The calculated power factor of these nanotubes can be optimized to much higher values in a wide temperature range. Using nonequilibrium molecule dynamics simulations, the lattice thermal conductivity of these nanotubes are predicated with quantum correction. Our calculations indicate that the (4,2) tube has relatively higher room temperature figure of merit (ZT value) compared with those of the (5,0) and (3,3) tubes. Moreover, the thermoelectric performance of these nanotubes can be greatly enhanced by surface design, formation of bundles, increasing the tube length, and so on, which significantly reduce the phonon and electron-derived thermal conductance.

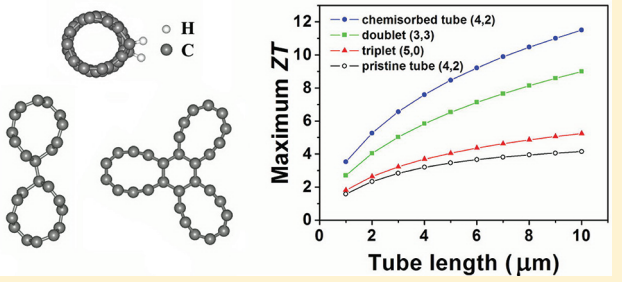

1. INTRODUCTION

Thermoelectric materials have attracted a lot of attention from the science community due to their interesting transport properties and potential applications in cooling and power generation. The efficiency of a thermoelectric material is given by the dimensionless figure of merit

$$ZT = \frac{S^2\sigma T}{(\kappa_e + \kappa_p)} \quad (1)$$

In this formula, S is the Seebeck coefficient, σ is the electrical conductivity, T is the absolute temperature, and κ_e and κ_p are the electron and phonon contributions to the thermal conductivity, respectively. Good thermoelectric materials behave as glass for phonons and crystal for electrons,[1] and one therefore must try to maximize the power factor ($S^2\sigma$) and minimize the thermal conductivity ($\kappa = \kappa_e + \kappa_p$). As these transport coefficients (S, σ, and κ) are coupled with each other and related to the crystal structure and carrier concentration, it is very difficult to significantly improve the thermoelectric performance of conventional materials, which has a highest ZT value of about 1.0.[2,3] In 1993, Hicks et al. theoretically predicated that by using low-dimensional or nanostructures, one could obtain ZT value much higher than that of the corresponding bulk materials.[4] The reason can be attributed to a reduction of κ_p by surface/interface phonon scattering, as well as the enhanced $S^2\sigma$ due to quantum confinement effect.

Among many nanostructures, carbon nanotubes (CNTs) have been extensively studied since their discovery in 1991.[5] It is, thus, nature to ask if CNTs can be used as thermoelectric materials. As ideal one-dimensional quantum wires, CNTs were found to exhibit ballistic electron transport,[6−10] and the reported electrical conductivity can be as high as 10^6∼10^8 S/m[11−15] at room temperature (RT). However, the results from both experimental measurements[11,16−19] and theoretical calculations[20−24] indicate that the RT thermal conductivity of CNTs are also very high (10^2∼10^4 W/m·K). This seems limit the thermoelectric application of CNTs. Indeed, most of previous works were focused on the measurement of Seebeck coefficient of CNTs, which have an absolute value ranging from tens to hundreds μV/K around RT.[19,25−29] Recently, Zhang et al.[30] fabricated CNT bulk samples by spark plasma sintering and found that the thermal conductivity can be decreased to 4.2 W/m·K at RT because of intensive tube−tube interactions. It is thus favorable to use them as thermoelectric materials that require low thermal conductivity but high electrical conductivity. Prasher et al.[31] also found that the strong tube−tube interactions in a random network of CNTs can lead to a significant reduction of the measured thermal conductivity. The ZT value of the so-called "CNT bed" structure was estimated to be 0.2 at RT, which is about 2 orders of magnitude larger than that of isolated CNTs. Using nonequilibrium Green's function approach, Jiang et al.[32] investigated the phonon and electron transports in the zigzag CNTs (n,0) with $mod\ (n,3) \neq 0$. The maximum ZT value they obtained is about

Received: June 7, 2011
Revised: September 23, 2011
Published: September 23, 2011

dx.doi.org/10.1021/jp205333m | J. Phys. Chem. C 2011, 115, 21996–22001

0.2 at RT. Although these pioneering works discussed the possibility of using CNTs as thermoelectric materials, the reported ZT value is still not comparable to that of the best commercial materials. In this work, we use a combination of nonequilibrium Green's function method and molecular dynamics simulation to study the thermoelectric properties of three kinds of ultrasmall single-wall carbon nanotubes, namely, the zigzag (5,0), the chiral (4,2), and the armchair (3,3). These nanotubes were fabricated by a templating method and have a diameter of about 0.4 nm,[33] probably at or close to the theoretical limit. We shall see that all these nanotubes could be optimized to exhibit much higher ZT value by significantly reducing the phonon and electron derived thermal conductance, which suggests their promising thermoelectric applications.

2. COMPUTATIONAL DETAILS

The electronic transport has been studied using the nonequilibrium Green's function (NEGF) method, as implemented in the Atomistix ToolKit (ATK) software package.[34,35] As usual, in the NEGF model, the nanotube is divided into a central part connected by the left and right semi-infinite ones. We focus on the ballistic transport, and the weak electron−phonon scattering is ignored. During the self-consistent calculations, we use the Troullier−Martins nonlocal pseudopotentials[36] to describe the electron−ion interactions. The exchange-correlation energy is in the form of PW91[37] and the Brillouin zone is sampled with $1 \times 1 \times 100$ Monkhorst-Pack k-mesh.[38] The mixing rate of electronic Hamiltonian is set to be 0.1, and the convergent criterion for the total energy is 4×10^{-5} eV. We use a double ζ basis set plus polarization for the carbon atoms and the cutoff energy is set as 150 Ry. On the other hand, the thermal transport is calculated using the reverse nonequilibrium molecular dynamics (NEMD) simulations implemented in the LAMMPS software package.[39] We adopt the Tersoff potential[40] and solve Newtonian equations of motion according to the Müller−Plathe algorithm[41] with a fixed time step of 0.55 fs. To make sure that the system has reached steady state, a constant temperature simulation of 700000 steps and a constant energy simulation of 300000 steps are carried out. The nanotubes are then divided into N equal segments with periodic boundary condition, and the segments at $N/4$ and $3N/4$ are defined as hot and cold regions, respectively. The kinetic energies are swapped between the coldest atom(s) in the hot region and the hottest one(s) in the cold region, then a temperature gradient responses and thermal flux maintains via atoms interactions in neighboring segments.[22,42] Our calculated results are carefully tested with respect to the number of divisions and time steps.

3. RESULTS AND DISCUSSIONS

We begin with the electronic transport of these 0.4 nm nanotubes. As mentioned before, we use a standard model where the central scattering region is connected by two semi-infinite electrodes that are also carbon nanotubes in the present study. To get reliable results, the length of the central part is carefully tested and contains 10, 2, and 6 unit cells for the (3,3), (4,2), and (5,0) tubes, respectively. Figure 1 shows the calculated transmission function $T(E)$ of these nanotubes under zero bias voltage. We see that all of them display a clear stepwise structure that gives the number of electron channels. The quantized transmission indicates ballistic transport of electrons in the carbon nanotubes, as suggested by previous studies. It should be mentioned that the

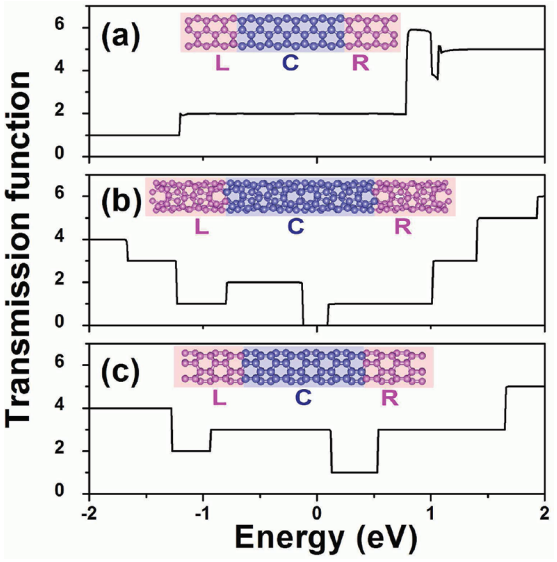

Figure 1. Transmission function of 0.4 nm carbon nanotubes: (a) armchair (3,3), (b) chiral (4,2), and (c) zigzag (5,0) under zero bias voltage. The insets are ball-and-stick models of these nanotubes that are divided into a central part connected by the left and right semi-infinite ones, as usually done in the NEGF approach.

transmission function of (4,2) tube vanishes around the Fermi level, which is consistent with the fact that among the 0.4 nm nanotubes, the (4,2) tube is the only semiconductor with a band gap of ~0.2 eV.[43]

Based on the calculated transmission function, the electronic transport coefficients can be readily obtained.[44] As the cross-sectional area is not well-defined for quasi-one-dimensional systems such as CNTs, we will discuss the conductance (G, λ_e, or λ_p)[45] instead of the conductivity (σ, κ_e, or κ_p) mentioned before. The dimensionless figure of merit is therefore rewritten as

$$ZT = \frac{S^2GT}{(\lambda_e + \lambda_p)} \tag{2}$$

Let

$$L_m(\mu) = \frac{2}{h}\int_{-\infty}^{\infty} dE T(E)(E-\mu)^m \left(-\frac{\partial f(E,\mu)}{\partial E}\right) \tag{3}$$

where $f(E,\mu)$ is the Fermi-Dirac distribution function, we can then, respectively, write the Seebeck coefficient, the electrical conductance, and the electronic thermal conductance as

$$S(\mu, T) = \frac{1}{eT}\frac{L_1(\mu)}{L_0(\mu)} \tag{4}$$

$$G(\mu, T) = e^2 L_0(\mu) \tag{5}$$

$$\lambda_e(\mu, T) = \frac{1}{T}\left\{L_2(\mu) - \frac{[L_1(\mu)]^2}{L_0(\mu)}\right\} \tag{6}$$

Figure 2 plots the redefined power factor (S^2G) as a function of chemical potential μ and temperature T for the (3,3), (4,2), and (5,0) tubes. As indicated in the color scale, the red and blue stand for large and small calculated values of S^2G, respectively. Note here the chemical potential determines the doping level of the system, and the positive and negative μ correspond to n-type and

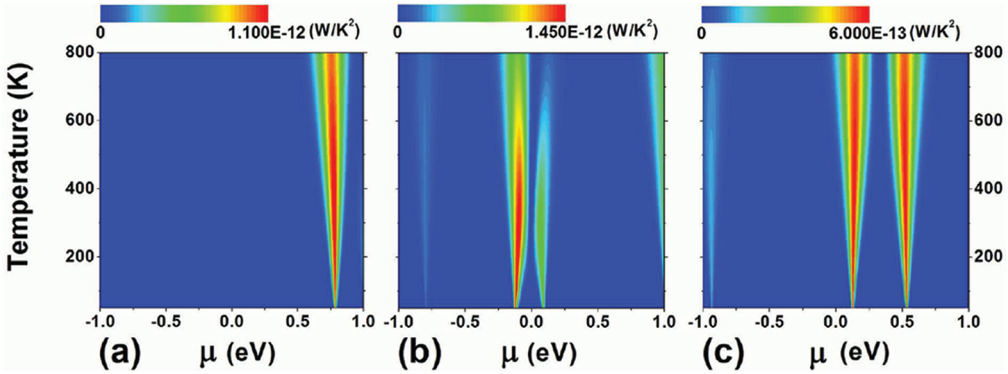

Figure 2. Calculated power factor S^2G of 0.4 nm carbon nanotubes: (a) (3,3), (b) (4,2), and (c) (5,0) as a function of chemical potential μ and temperature T.

Table 1. Optimized ZT Value at 300 K for the 0.4 nm Carbon Nanotubes (3,3), (4,2), and (5,0)[a]

tube	μ (eV)	S^2G (W/K^2)	λ_e (nW/K)	λ_p (nW/K)	κ_p (W/ m·K)	ZT
(3,3)	0.78	1.11×10^{-12}	1.89	0.21	1615	0.16
(4,2)	−0.09	1.39×10^{-12}	0.08	0.18	1330	1.6
(5,0)	0.53	5.81×10^{-13}	0.96	0.30	2073	0.14

[a] The tube length is assumed to be 1 μm. The corresponding chemical potential μ, the power factor S^2G, the electronic thermal conductance λ_e, and the lattice thermal conductance λ_p and conductivity κ_p are also indicated.

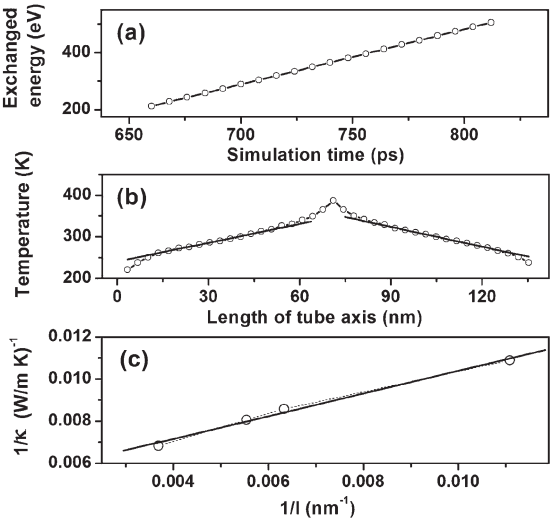

Figure 3. (a) Typical time variation of the exchanged kinetic energy for the (4,2) tube; (b) Typical temperature profile for the (4,2) tube at an average temperature of 300 K; (c) The inverse thermal conductivity $1/\kappa_p$ as a function of inverse tube length $1/l$, where the open circles represent explicit MD results and the solid line indicates a linear fit.

p-type doping, respectively. As can be seen from Figure 2, the calculated power factor exhibit one or two highlight areas with obviously large values in a wide temperature range. This observation suggests that one can always enhance the thermoelectric performance of these nanotubes by appropriate n-type and p-type doping. If we focus on the room temperature, we find from Table 1 that the (4,2) and (3,3) tubes have relatively large value

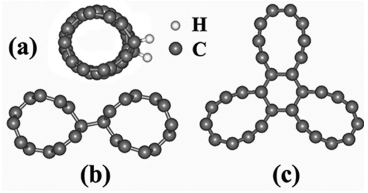

Figure 4. Top-view of the fully relaxed structures for (a) the (4,2) tube chemisorbed with two hydrogen atoms, (b) the doublet bundle of (3,3) tube, and (c) the triplet bundle of (5,0) tube.

of S^2G compared with that of the (5,0) tube. However, the much higher electronic thermal conductance λ_e makes the pristine (3,3) tube less possible for the thermoelectric applications. The most favorable candidate should be (4,2) tube, which has a very small λ_e but larger S^2G with chemical potential close to the Fermi level.

We now move to the discussion of phonon transport by using the NEMD simulation, which can handle anharmonicity and turns out to be an efficient approach to calculate thermal conductivity as long as the temperature is not very low. In the present work, the nanotubes are divided into 40 equal segments, and the first (21th) one is set as cold (hot) region. One atom in each region exchange their kinetic energy every 80 time steps and others interact to reach a quasi-equilibrium state until the next exchange happens. Figure 3a shows the exchanged kinetic energy as a function of simulation time for the (4,2) tube at 300 K. The simulation cell is about 135 nm in length. We see that the exchanged energy increases linearly in the whole simulation time, which suggests a stable heat flux J from the hot to cold region. As shown in Figure 3b, there is a linear temperature response along the tube axis except for the middle hot region and outer cold region. The temperature gradient ∇T is thus obtained by averaging the slope values of two linearly fitted lines shown in Figure 3b. Inserting these values into the Fourier's law

$$\kappa_p = \frac{J}{(A \cdot \nabla T)} \tag{7}$$

the phonon-derived thermal conductivity κ_p can be calculated. Here A is the cross-sectional area for low-dimensional systems such as CNTs. A proper treatment is using the thermal conductance λ_p,[45] which is related to the thermal conductivity by

$$\lambda_p = \kappa_p A/l \tag{8}$$

Table 2. Optimized *ZT* Value at 300 K for the Chemisorbed (4,2) Tube, the Doublet Bundle of (3,3) Tube, and the Triplet Bundle of (5,0) Tube[a]

structure	μ (eV)	S^2G (W/K^2)	λ_e (nW/K)	λ_p (nW/K)	κ_p (W/ m·K)	*ZT*
tube (4,2) + H_2	0.81	1.24×10^{-12}	0.038	0.067	281	3.5
doublet (3,3)	0.79	3.22×10^{-12}	0.13	0.23	885	2.7
triplet (5,0)	0.24	2.49×10^{-12}	0.14	0.27	622	1.8

[a] The tube length is assumed to be 1 μm. The corresponding chemical potential μ, the power factor S^2G, the electronic thermal conductance λ_e, and the lattice thermal conductance λ_p and conductivity κ_p are also indicated.

where l is the length of CNTs and in the order of micrometer size for most carbon nanotube samples.

It is well-known that the thermal conductivity κ_p of bulk materials is only determined by their composite and is size independent. This is however not the case for low-dimensional systems. Both experiment measurement[29] and MD simulations[20,46] indicate that the thermal conductivity of CNTs are related to their length. As most thermal energy is transported by acoustic phonons that scatter at the boundary of the tubes and the phonon mean free path is limited by the size of the simulation cell, the thermal conductivity increases with increasing tube length within the ballistic transport regime. When the transport extends to the diffusive regime, the thermal conductivity diverges as $\kappa_p \sim l^\beta$, where the exponent β depends on the temperature and tube length l. To obtain a fully diffusive thermal conductivity of our systems, the κ_p with different tube lengths are calculated and extrapolated to obtain a good estimate at infinite length. A simple approach of effective phonon travel path l_{eff} is given by

$$1/l_{eff} = 1/l_\infty + 4/l \quad (9)$$

where l is the length of simulated CNTs, l_∞ is the phonon mean free path for infinite system, and the factor 4 means that phonons will be at an average distance $l/4$ from either the cold region or the hot one where the last anharmonic scattering event occurred.[42] This formula suggests that a plot of $1/\kappa_p$ versus $1/l$ should be linear and that the thermal conductivity of CNTs at any length can thus be calculated. Figure 3c gives the results for the (4,2) tube, where the solid line is fitted from the $1/\kappa_p$ at a series of tube length. If the tube has a typical length of 1 μm, the thermal conductivity can be readily obtained by extrapolating to $1/l = 0.001$ nm^{-1}.

It should be mentioned that, in our MD simulation, the temperature is defined by the formula

$$\langle E \rangle = \sum_{i=1}^{N} \frac{1}{2} m v_i^2 = \frac{3}{2} N k_B T_{MD} \quad (10)$$

where $\langle E \rangle$ is the mean kinetic energy, N is the number of atoms in the simulation cell, m is the atomic mass, v_i is the velocity of atom i, and k_B is the Boltzmann constant. However, this formula is valid only when the temperature is higher than the Debye temperature Θ_D. If we are interested in the room or intermediate temperature region, which is lower than the Θ_D of CNTs (usually 500−1000 K), a quantum correction to both the MD temperature and the thermal conductivity must be carried out. This is done by redefining the MD temperature as[47]

$$3Nk_B T_{MD} = \int_0^{\omega_\Theta} D(\omega) n(\omega, T) \hbar\omega \, d\omega \quad (11)$$

where $D(\omega)$ is the phonon density of states obtained from density functional perturbation theory, $n(\omega,T)$ is the Bose−Einstein distribution, and ω_Θ is the Debye frequency. The quantum corrected thermal conductivity κ_p as well as the thermal conductance λ_p for the 0.4 nm nanotubes at 300 K are summarized in Table 1, where the tube length is assumed to be 1 μm. We find these three kinds of nanotubes have quite different thermal conductivity although they are nearly of the same diameter. It is generally accepted that the acoustic branches play a significant role in the thermal conductivity of carbon nanotubes.[48] As the calculated heat capacity and the phonon group velocity of those 0.4 nm nanotubes are more or less similar to each other, we believe that the large difference in the thermal conductivity (or thermal conductance) is mainly due to their different phonon mean free path.

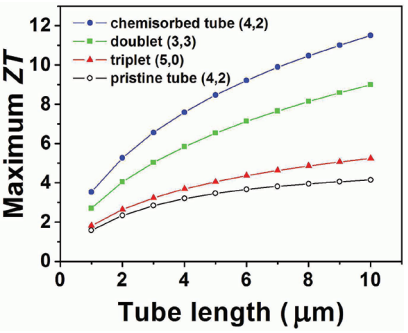

Figure 5. Optimized *ZT* value at 300 K as a function of tube length for the pristine (4,2) tube, the (4,2) tube with chemisorbed hydrogen, the triplet bundle of (5,0) tube, and the doublet bundle of (3,3) tube.

Based on the calculated power factor S^2G, the electronic thermal conductance λ_e, and the phonon-induced thermal conductance λ_p, we are able to evaluate the figure of merit according to eq 2. Due to relatively larger S^2G and smaller λ_e and λ_p (see Table 1), we find that the (4,2) tube has the highest *ZT* value among the three kinds of 0.4 nm tubes, which is 1.6 (at length of 1 μm) at room temperature. This value is already larger than those reported previously for larger diameter carbon nanotubes or their composites.[31,32,49] We further find that chemisorptions of hydrogen on the (4,2) tube could result in a significant reduction of both the λ_p and λ_e, while maintaining good power factor S^2G. For the optimized product where two hydrogen atoms chemisorbed on top of the C−C bond that has the lowest angle with the tube axis (see Figure 4a), we see from Table 2 that the calculated λ_p (λ_e) is only 0.067 nW/K (0.038 nW/K) compared with 0.18 nW/K (0.08 nW/K) of the pristine (4,2) tube. The maximum *ZT* value of the chemisorbed (4,2) tube is, thus, increased to 3.5, which is comparable to that of the best commercial materials.

In addition to the surface design mentioned above, we find that formation of carbon nanotube bundles could also give an

improved ZT value. Here we consider two examples, namely, the doublet (3,3) and the triplet (5,0). In contrast to the weak tube−tube interactions found in a bundle of large diameter nanotubes, the ultrasmall tubes within the doublet and triplet bundles are covalently connected,[50] as shown in Figure 4b,c. Our MD simulations indicate that such new forms of bundle are energetically favorable and kinetically stable around room temperature. Due to very strong tube−tube interactions, we see from Tables 1 and 2 that the electronic thermal conductance λ_e is lowered by 93% for the doublet (3,3), and 85% for the triplet (5,0). Moreover, there is an obvious increase of the corresponding power factor S^2G and a decrease of the phonon derived thermal conductivity κ_P. As a result, the calculated ZT value increases significantly from 0.14 to 1.8 for the triplet (5,0), and from 0.16 to 2.7 for the doublet (3,3).

It should be emphasized that we have assumed the tube length is 1 μm in the above discussions. This is not necessarily the case for a real system where the tube length varies from sample to sample. As the thermal conductance λ_P will decrease with increasing tube length, our calculated ZT values may further increase as obviously shown in Figure 5. For example, the ZT value of pristine and hydrogen adsorbed (4,2) tube with length of 3 μm can be, respectively, enhanced to 2.8 and 6.6 at optimized chemical potential. Similar trends can be found for the carbon nanotube bundles, which has a ZT value of 4.1 for the triplet (5,0), and 6.5 for the doublet (3,3) when the bundle length is 5 μm. If the sample length is further increased to 10 μm, we see from Figure 5 that the predicated ZT value can be as high as 11.5 for the (4,2) tube chemisorbed with hydrogen. The significantly enhanced ZT values suggest very favorable thermoelectric applications of these 0.4 nm carbon nanotubes.

4. SUMMARY

In summary, the thermoelectric properties of three kinds of ultrasmall diameter carbon nanotubes are studied by using nonequilibrium Green's function method and molecule dynamics simulations. Our calculated results indicate that, although these nanotubes do not have much higher ZT value in the pristine form, their thermoelectric performance can be significantly enhanced via surface design, formation of bundles, increasing the tube length, and so on. It is, thus, reasonable to expect that these carbon nanotubes could be very promising thermoelectric material, which needs further experimental and theoretical investigations.

AUTHOR INFORMATION

Corresponding Author

*E-mail: phlhj@whu.edu.cn; jshi@whu.edu.cn.

ACKNOWLEDGMENT

This work was supported by the "973 Program" of China (Grant No. 2007CB607501), the National Natural Science Foundation (Grant No. 51172167), and the Program for New Century Excellent Talents in University. We also acknowledge financial support from the interdiscipline and postgraduate programs under the "Fundamental Research Funds for the Central Universities". All the calculations were performed in the PC Cluster from Sugon Company of China.

REFERENCES

(1) Slack, G. A. In *CRC Handbook of Thermoelectrics*; Rowe, D. M., Ed.; CRC Press: Boca Raton, 1995; p 407.
(2) Tritt, T. *Science* **1999**, *283*, 804.
(3) DiSalvo, F. J. *Science* **1999**, *285*, 703.
(4) Hicks, L. D.; Dresselhaus, M. S. *Phys. Rev. B* **1993**, *47*, 12727. and *ibid***1993**, *47*, 16631.
(5) Iijima, S. *Nature* **1991**, *354*, 56.
(6) Tans, S. J.; Devoret, M. H.; Dai, H.; Thess, A.; Smalley, R. E.; Geerligs, L. J.; Dekker, C. *Nature* **1997**, *386*, 474.
(7) White, C. T.; Todorov, T. N. *Nature* **1998**, *393*, 240. and *ibid***2001**, *411*, 649.
(8) Bachtold, A.; Fuhrer, M. S.; Plyasunov, S.; Forero, M.; Anderson, E. H.; Zettl, A.; McEuen, P. L. *Phys. Rev. Lett.* **2000**, *84*, 6082.
(9) Kong, J.; Yenilmez, E.; Tombler, T. W.; Kim, W.; Dai, H.; Laughlin, R. B.; Liu, L.; Jayanthi, C. S.; Wu, S. Y. *Phys. Rev. Lett.* **2001**, *87*, 106801.
(10) Javey, A.; Guo, J.; Wang, Q.; Lundstrom, M.; Dai, H. *Nature* **2003**, *424*, 654.
(11) Hone, J.; Llaguno, M. C.; Nemes, N. M.; Johnson, A. T.; Fischer, J. E.; Walters, D. A.; Casavant, M. J.; Schmidt, J.; Smalley, R. E. *Appl. Phys. Lett.* **2000**, *77*, 666.
(12) DUrkop, T.; Getty, S. A.; Cobas, E.; Fuhrer, M. S. *Nano Lett.* **2004**, *4*, 35.
(13) Wescott, J. T.; Kung, P.; Maiti, A. *Appl. Phys. Lett.* **2007**, *90*, 033116.
(14) Purewal, M. S.; Hong, B. H.; Ravi, A.; Chandra, B.; Hone, J.; Kim, P. *Phys. Rev. Lett.* **2007**, *98*, 186808.
(15) Ishii, H.; Kobayashi, N.; Hirose, K. *Phys. Rev. B* **2010**, *82*, 085435.
(16) Hone, J.; Whitney, M.; Piskoti, C.; Zettl, A. *Phys. Rev. B* **1999**, *59*, R2514.
(17) Kim, P.; Shi, L.; Majumdar, A.; McEuen, P. L. *Phys. Rev. Lett.* **2001**, *87*, 215502.
(18) Yu, C.; Shi, L.; Yao, Z.; Li, D.; Majumdar, A. *Nano Lett.* **2005**, *5*, 1842.
(19) Pop, E.; Mann, D.; Cao, J.; Wang, Q.; Goodson, K.; Dai, H. *Phys. Rev. Lett.* **2005**, *95*, 155505.
(20) Che, J.; Çağın, T.; Goddard, W. A., III *Nanotechnology* **2000**, *11*, 65.
(21) Berber, S.; Kwon, Y. K.; Tománek, D. *Phys. Rev. Lett.* **2000**, *84*, 4613.
(22) Osman, M. A.; Srivastava, D. *Nanotechnology* **2001**, *12*, 21.
(23) Cao, J. X.; Yan, X. H.; Xiao, Y.; Ding, J. W. *Phys. Rev. B* **2004**, *69*, 073407.
(24) Gu, Y.; Chen, Y. *Phys. Rev. B* **2007**, *76*, 134110.
(25) Hone, J.; Ellwood, I.; Muno, M.; Mizel, A.; Cohen, M. L.; Zettl, A.; Rinzler, A. G.; Smalley, R. E. *Phys. Rev. Lett.* **1998**, *80*, 1042.
(26) Sumanasekera, G. U.; Adu, C. K. W.; Fang, S.; Eklund, P. C. *Phys. Rev. Lett.* **2000**, *85*, 1096.
(27) Barišić, N.; Gaál, R.; Kézsmárki, I.; Mihály, G.; Forró, L. *Phys. Rev. B* **2002**, *65*, R241403.
(28) Small, J. P.; Perez, K. M.; Kim, P. *Phys. Rev. Lett.* **2003**, *91*, 256801.
(29) Chang, C. W.; Okawa, D.; Garcia, H.; Majumdar, A.; Zettl, A. *Phys. Rev. Lett.* **2008**, *101*, 075903.
(30) Zhang, H. L.; Li, J. F.; Yao, K. F.; Chen, L. D. *J. Appl. Phys.* **2005**, *97*, 114310.
(31) Prasher, R. S.; Hu, X. J.; Chalopin, Y.; Mingo, N.; Lofgreen, K.; Volz, S.; Cleri, F.; Keblinski, P. *Phys. Rev. Lett.* **2009**, *102*, 105901.
(32) Jiang, J. W.; Wang, J. S.; Li, B. *J. Appl. Phys.* **2011**, *109*, 014326.
(33) Wang, N.; Tang, Z. K.; Li, G. D.; Chen, J. S. *Nature* **2000**, *408*, 50.
(34) Brandbyge, M.; Mozos, J. L.; Ordejón, P.; Taylor, J.; Stokbro, K. *Phys. Rev. B* **2002**, *65*, 165401.
(35) Soler, J. M.; Artacho, E.; Gale, J. D.; García, A.; Junquera, J.; Ordejón, P.; Sánchez-Portal, D. *J. Phys.: Condens. Matter* **2002**, *14*, 2745.

(36) Troullier, N.; Martins, J. L. *Phys. Rev. B* **1991**, *43*, 8861.
(37) Perdew, J. P.; Wang, Y. *Phys. Rev. B* **1992**, *45*, 13244.
(38) Monkhorst, H. J.; Pack, J. D. *Phys. Rev. B* **1976**, *13*, 5188.
(39) Plimpton, S.; , *J. Comput. Phys.* **1995**, *117*, 1. Code available at: http://lammps.sandia.gov/download.html.
(40) Tersoff, J. *Phys. Rev. B* **1989**, *39*, 5566.
(41) Müller-Plathe, F. *J. Chem. Phys.* **1997**, *106*, 6082.
(42) Schelling, P. K.; Phillpot, S. R.; Keblinski, P. *Phys. Rev. B* **2002**, *65*, 144306.
(43) Liu, H. J.; Chan, C. T. *Phys. Rev. B* **2002**, *66*, 115416.
(44) Esfarjani, K.; Zebarjadi, M.; Kawazoe, Y. *Phys. Rev. B* **2006**, *73*, 085406.
(45) Alaghemandi, M.; Algaer, E.; Böhm, M. C.; Müller-Plathe, F. *Nanotechnology* **2009**, *20*, 115704.
(46) Huang, Z. X.; Tang, Z. A. *Phys. B* **2006**, *373*, 291.
(47) Maiti, A.; Mahan, G. D.; Pantelides, S. T. *Solid State Commun.* **1997**, *102*, 517.
(48) Donadio, D.; Galli, G. *Phys. Rev. Lett.* **2007**, *99*, 255502. and *ibid***2009**, *103*, 149901.
(49) Kim, D.; Kim, Y.; Choi, K.; Grunlan, J. C.; Yu, C. *ACS Nano* **2010**, *4*, 513.
(50) Wen, Y. W.; Liu, H. J.; Pan, L.; Tan, X. J.; Lv, H. Y.; Shi, J.; Tang, X. F. *J. Phys. Chem. C* **2011**, *115*, 9227.